

# A thermal bimorph micromirror with large bi-directional and vertical actuation

Ankur Jain\*, Hongwei Qu, Shane Todd, Huikai Xie

*Department of Electrical and Computer Engineering, University of Florida, 136 Larsen Hall, P.O. Box 116200, Gainesville, FL 32611-6200, USA*

Available online 3 March 2005

## Abstract

This paper reports a novel large vertical displacement (LVD) microactuator that can generate large piston motion and bi-directional scanning at low driving voltage. A LVD micromirror device has been fabricated by using a unique deep reactive ion etch (DRIE) post-CMOS micromachining process that simultaneously provides thin-film and single-crystal silicon microstructures. The bimorph actuation structure is composed of aluminum and silicon dioxide with an embedded polysilicon thermal resistor. With a size of only 0.7 mm × 0.32 mm, the LVD micromirror demonstrated a vertical displacement of 0.2 mm at 6 V dc. This device can also be used to perform bi-directional rotational scanning through the use of two bimorph actuators. The micromirror rotates over ±15° at less than 6 V dc, and over ±43° (i.e., >170° optical scan angle) at its resonant frequency of 2.6 kHz.

© 2005 Elsevier B.V. All rights reserved.

*Keywords:* Bi-directional scanning; Electrothermal actuation; Large rotation angle; Large vertical displacement; Microactuators; Optical scanner; Vertical actuation

## 1. Introduction

Scanning micromirrors have been demonstrated for a wide variety of applications such as for optical displays [1,2], biomedical imaging [3,4], laser beam steering [5], and optical switching [6]. The advantages of using micromirrors over conventional scanning solutions include their small size, high speed, low power consumption, and the potential for low cost through batch fabrication. Fast-scanning mirrors that can generate piston motion are required by applications for wavefront shaping in adaptive optics [7], interferometry systems [8], and spatial light modulators [9]. Other applications that require large vertical displacements include tunable lenses for confocal microscopy [10], microvalves [11], actuators on magnetic recording heads, and precision micropositioning systems [12].

Another promising application for large piston motion micromirrors is in optical coherence tomographic (OCT) imaging systems. OCT is a non-destructive biomedical imaging technology that produces high-resolution cross-sectional im-

ages of biological tissue [13]. The core of an OCT system is a Michelson interferometer in which a broadband light beam is split into a reference arm and a sample arm. The reflected light beams from the reference mirror and the sample interfere with each other. The interference, which occurs only when the optical path difference is within the coherence length of the light source, is picked up by the photodetector. Therefore, the coherence length determines the axial resolution, and the axial scanning of the reference mirror generates cross-sectional images. Typically, imaging depth of about 2 mm in tissue samples is required, so the optical delay line in the reference arm must perform axial scanning by a few millimetres [14]. Various methodologies have been proposed to generate that large optical delay. For example, some research groups have simply used the translation of a reference mirror mounted on a stage driven by a dc motor or voice coil for axial scanning [13], while others have used a piezoelectric transducer to drive a parallel mirror system in which light is reflected multiple times [15]. Other more complicated delay lines achieve faster axial scans by using rapid scanning optical delay (RSOD) scanning systems that use a combination of a grating, lens, and scanning mirror [16]; or by using three different reflecting mirrors [17]. Optical delay

\* Corresponding author. Tel.: +1 352 392 1049; fax: +1 352 846 1416.  
E-mail addresses: [ajain@ufl.edu](mailto:ajain@ufl.edu) (A. Jain); [hkxie@ece.ufl.edu](mailto:hkxie@ece.ufl.edu) (H. Xie).

lines based on piston motion micromirrors can potentially reduce the size and complexity of OCT systems, and increase the imaging speed as well.

Numerous piston motion actuation designs have been reported in literature. Vertical displacements of  $7.5\ \mu\text{m}$  [18] and even as high as  $55\ \mu\text{m}$  [10] have been achieved through the use of electrostatic vertical comb drives. Deformable mirrors with electromagnetic and electrostatic actuations for use in adaptive optics demonstrated vertical displacements of  $20\ \mu\text{m}$  [19] and  $6\ \mu\text{m}$  [7], respectively. Other vertical actuation mechanisms include a piezoelectric cantilever with displacements up to  $25\ \mu\text{m}$  [20], and an electrothermally actuated trampoline-type micromirror with a maximum displacement of  $2\ \mu\text{m}$  [21]. These above-mentioned actuators generate vertical displacements only up to a few tens of microns, and therefore are not suitable for OCT axial scanning.

In this paper, we present a novel micromirror design, which has the potential to meet the axial-scanning requirements of OCT systems. In prior research, we demonstrated single-crystal silicon (SCS) based one-dimensional and two-dimensional scanning micromirrors with large rotation angle for transverse scanning in OCT imaging [22,23]. These mirrors used aluminum/silicon dioxide bimorph beams with an embedded polysilicon heater for electrothermal actuation. The unidirectional operation, non-stationary center of rotation, and large initial tilt angle of those micromirrors complicated the device packaging and optical design. Using the same actuator design concepts, we have developed a novel large vertical displacement (LVD) micromirror design that can perform bi-directional optical scans and generate large piston motion at low driving voltages [24,25]. This device uses two complementary bimorph actuators, which are oriented in a folded structure to keep the mirror plate parallel to the substrate plane. It is well known that there is large  $z$ -displacement at the tip of a long rotational beam. The in-

novation of this LVD device is converting the large tip displacement into a pure  $z$ -axis displacement of a flat micromirror. The LVD microactuator design can potentially achieve maximum vertical displacements of a few millimeters with millimeter-sized devices. Since this device can also perform bi-directional scans, it can also be used in the sample arm of an endoscopic OCT system to transversely scan the tissue surface. This micromirror is fabricated using a deep reactive ion etch (DRIE) post-CMOS micromachining process [26] that can simultaneously provide thin-film beams and single-crystal silicon microstructures.

In this paper, the LVD concept, device design, and fabrication process are described first. Then the experimental results, including frequency response, piston motion, and bi-directional scanning, are reported.

## 2. LVD micromirror design

The schematic drawing of the LVD micromirror is illustrated in Fig. 1. The mirror plate is attached to a rigid silicon frame by a set of aluminum/silicon dioxide bimorph beams. A polysilicon resistor is embedded within the silicon dioxide layer to form the heater for thermal bimorph actuation. As this set of beams directly actuates the mirror, it is referred to as the *mirror actuator*. The movable frame is connected to the silicon substrate by another set of identical bimorph beams. This second set of beams actuates the frame, and is referred to as the *frame actuator*. Each side of the rectangular frame is  $40\ \mu\text{m}$  wide, and has a  $40\ \mu\text{m}$  thick single-crystal silicon layer under it to provide rigidity to the structure. After the mirror is released during fabrication, the bimorph beams curl up due to the tensile stress in the upper aluminum layer and compressive residual stress in the bottom silicon dioxide layer, as illustrated in Figs. 1 and 2. The rigidity of the

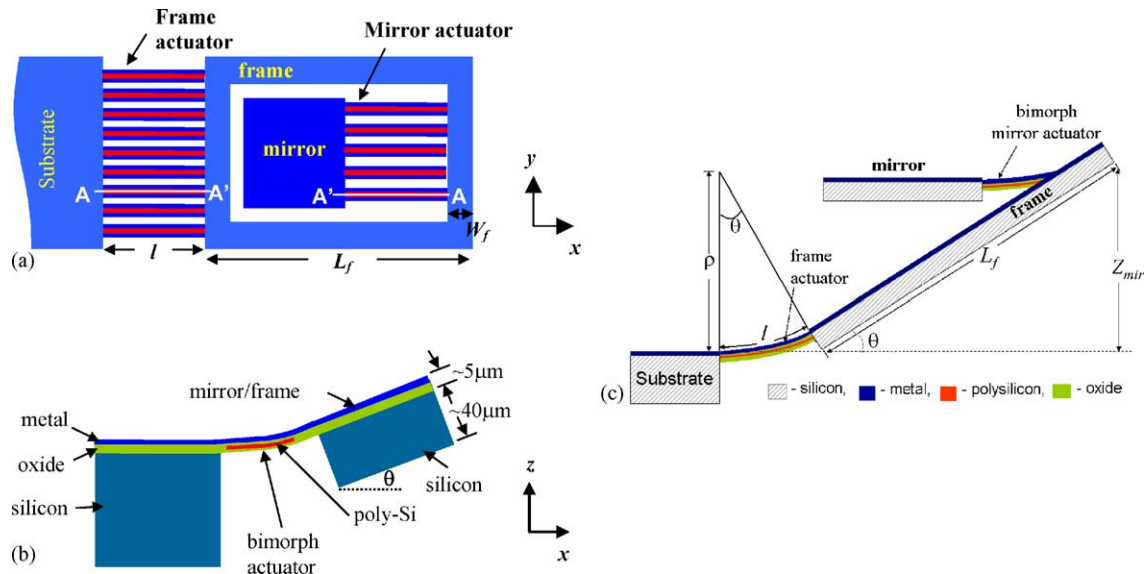


Fig. 1. Design schematic of the LVD micromirror: (a) top view; (b) cross-sectional view of A-A'; (c) cross-sectional view of the LVD device.

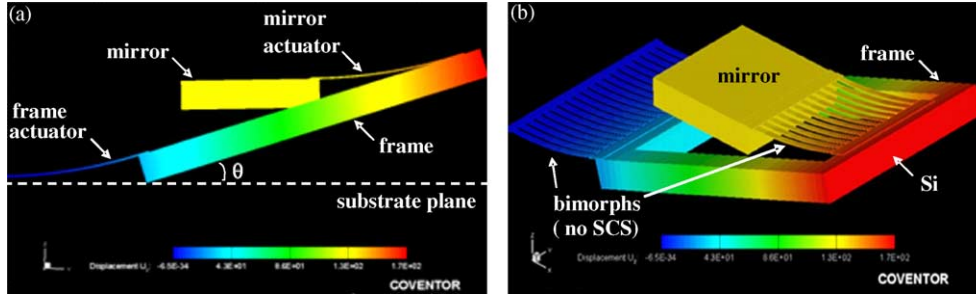


Fig. 2. (a) Side-view and (b) 3D model of the LVD micromirror illustrating the initial curling of the bimorph actuators. The mirror surface is parallel to the substrate plane, i.e. no initial tilt, as the curling of the two bimorph actuators compensate each other.

frame and the flatness of the mirror are guaranteed by the thick SCS layer underneath the frame and mirror. In contrast, the bimorph actuators do not have the SCS layer, and thus are thin and compliant in the  $z$ -direction. The mirror surface is coated with aluminum for broadband and high reflectivity. The fabrication details are given in the next section.

Finite element thermomechanical simulation was conducted using CoventorWare [27]. The simulation result is shown in Fig. 2, where the curls of the two sets of bimorph beams compensate each other resulting in a zero initial tilt. The initial elevation of the mirror plate above the chip plane,  $Z_{\text{mir}}$ , due to the curling of the thermal actuators can be calculated from:

$$Z_{\text{mir}} = (L_f - W_f) \sin \theta$$

where  $L_f$  and  $W_f$  are the length and beam width of the frame, respectively, and  $\theta$  is the initial tilt angle of the frame, which can be computed from  $\theta = l/\rho$ , where  $l$  and  $\rho$  are the length and radius of curvature of the thermal actuator, respectively. For a frame with  $L_f = 0.5$  mm,  $W_f = 40$   $\mu\text{m}$ , and  $\theta = 17^\circ$ , the initial rest position of the mirror  $Z_{\text{mir}}$  is 135  $\mu\text{m}$ . The simulation results in Fig. 2 show that the mirror plate is located 132  $\mu\text{m}$  above and parallel to the substrate plane. There is no substrate underneath the mirror plate. Thus, the mirror plate can move down below the chip surface plane. From experiment, it was found that the maximum displacement below the chip plane is roughly equal to  $Z_{\text{mir}}$ , thereby resulting in a maximum  $z$ -displacement,  $Z_{\text{max}} = 2Z_{\text{mir}} = 270$   $\mu\text{m}$ . Much larger vertical displacements can be achieved by simply increasing the frame and/or the actuator lengths.

The mirror and frame actuators rotate the mirror in opposite angular directions. There exist two basic modes of operation:

- Bi-directional scanning by alternatively applying voltage to the mirror and frame actuators.
- Large piston motion by simultaneously applying voltage to both actuators.

Equal angular rotations by the two actuators will result in pure vertical displacement of the mirror. Large  $z$ -axis displacement is achieved via the angular amplification due to the long arm length of the frame.

### 3. Device fabrication

The micromirror is fabricated using a DRIE CMOS-MEMS processing [26]. The post-CMOS process flow, outlined in Fig. 3, uses only four dry etch steps and can produce mixed thin-film and bulk-Si microstructures. The Agilent 0.5- $\mu\text{m}$  3-metal CMOS process available through the MOSIS foundry service [28] is used for the CMOS fabrication.

The post-CMOS process starts with a backside deep anisotropic silicon etch to form a 40- $\mu\text{m}$  thick SCS membrane in a surface technology systems (STS) ICP etcher. The etching chemistry used is  $\text{SF}_6/\text{O}_2$  with the following parameters: 600 W coil power, 12 W platen power, 130 sccm  $\text{SF}_6$  flow, 13 sccm  $\text{O}_2$  flow, and 37 mT chamber pressure. The 40- $\mu\text{m}$  thick SCS membrane is required to keep the mirror flat. The second step is a frontside anisotropic oxide etch that uses the CMOS interconnect metal (i.e. aluminum) as an etching mask. This oxide RIE etch is performed in a Unaxis Shuttle-

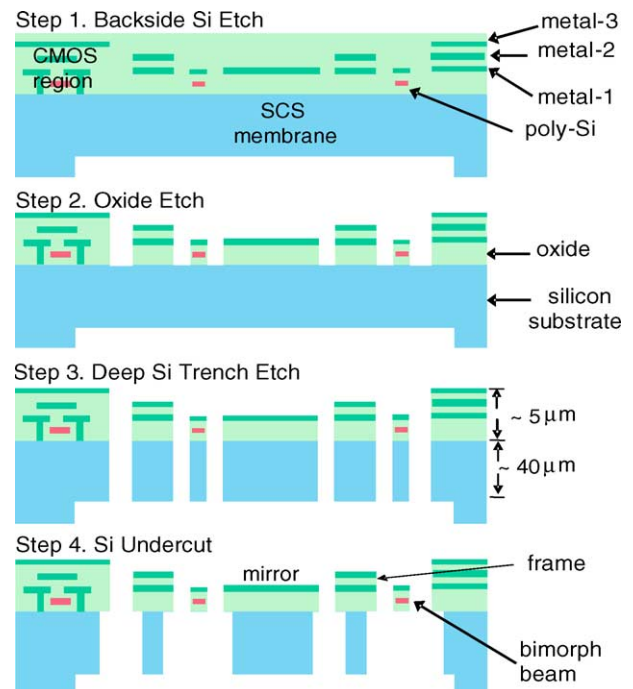


Fig. 3. DRIE CMOS-MEMS process flow.

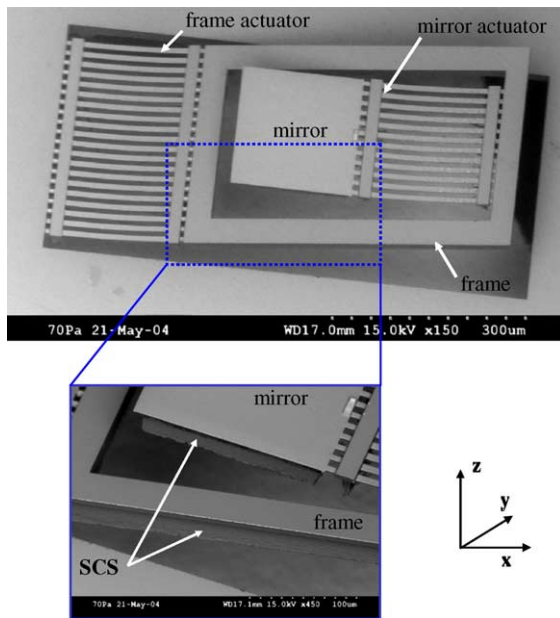


Fig. 4. SEM images of the LVD micromirror.

lock ICP etcher with the following process conditions: 600 W coil power, 100 W platen power, 15 sccm  $\text{SF}_6$  flow, 5 sccm Ar flow, and a chamber pressure of 5 mT. Next, a deep silicon trench etch is used to release the microstructure. The last step is an isotropic silicon etch to undercut the silicon to form thin-film bimorph beams which are approximately  $2\ \mu\text{m}$  thick. The isotropic silicon etch is attained using the STS etcher by reducing the platen power to 2 W. The thin-film beams provide z-axis compliance for out-of-plane actuation, and form bimorph actuators with an embedded polysilicon heater. As the top aluminum layer is used as an etching mask, CMOS circuits under it will remain unaffected by the fabrication process. Thus, this maskless post-CMOS process is completely compatible with foundry CMOS processes, and CMOS circuits can be integrated with MEMS devices.

A fabricated  $0.7\ \text{mm} \times 0.32\ \text{mm}$  LVD micromirror device is shown in Fig. 4. The initial tilt angle of the mirror plate in fabricated devices was less than  $0.5^\circ$ . The initial tilt angle of the frame with respect to the substrate surface is typically  $17^\circ$ . This tilt angle is dependent on the overetch of the top aluminum layer of the bimorph beams. The heating element in the  $10\text{-}\mu\text{m}$  wide bimorph beams is a set of  $200\text{-}\mu\text{m}$  long,  $7\text{-}\mu\text{m}$  wide polysilicon strips oriented along the beams. The gaps between the beams are  $9\ \mu\text{m}$  and are used to undercut the silicon underneath to form the thin-film bimorph beams. The frame actuator and mirror actuator are constituted of 20 and 12 bimorph beams, respectively. The measured open circuit polysilicon resistances of the mirror and frame actuators are 240 and  $365\ \Omega$ , respectively.

The mirror plate is  $190\ \mu\text{m} \times 190\ \mu\text{m}$ . This small mirror size is just used to demonstrate the proof of concept. Since the mirror plate is supported by bulk silicon, much larger mirrors can be made. The quality of the mirror surface was

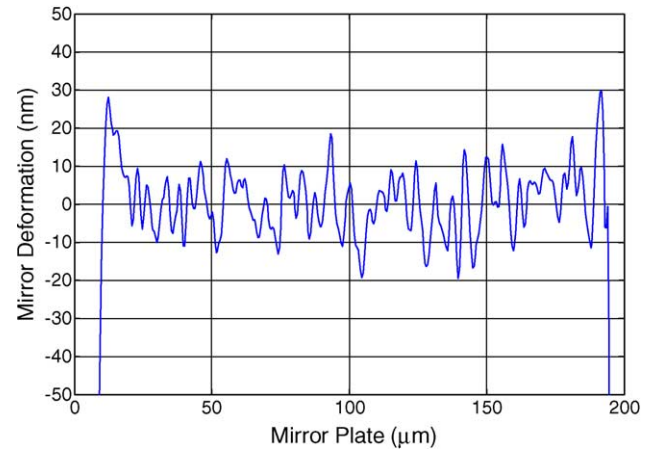


Fig. 5. Line scan of mirror surface deformations using a white light profilometer.

determined using a Wyko NT1000 white-light optical profilometer. A line scan of surface heights across the mirror plate is shown in Fig. 5. The peak-to-valley surface deformations are within 40 nm over the  $190\ \mu\text{m}$  mirror plate. The optical quality of the mirror is better than  $\lambda/20$  for near-infrared light.

## 4. Experimental results

Various experiments were performed to characterize the bi-directional rotation and piston motion scanning modes of a fabricated LVD micromirror device. Both dynamic and static responses were characterized to determine the rotation properties of the micromirror. The obtained characterization data was used to generate piston motion with negligible tilting of the mirror plate.

### 4.1. Bi-directional scanning

To determine the static response of the micromirror, an experimental setup with a laser beam incident on the mirror and a varying dc voltage applied to the two actuators was used to measure the static deflection angles. The mechanical dc scan angle of the mirror was obtained by measuring the displacement of the reflected laser beam on a calibrated screen. The mirror has a maximum rotation of  $26.5^\circ$  when 3 V dc (or 7 mA, corresponding to an applied power of 21 mW) is applied to the mirror actuator. Both the mirror and the frame rotate when a voltage is applied only to the frame actuator due to thermal coupling. A maximum deflection of  $-16.5^\circ$  is observed when 5.5 V dc (or 9 mA, corresponding to an electrical power of 50 mW) is applied to the frame actuator. As shown in Fig. 6, the rotation angles of the actuators vary linearly with applied voltage.

The same actuation voltage causes a larger rotation angle by the mirror actuator than the frame actuator due to the polysilicon resistance difference between the two actuators,

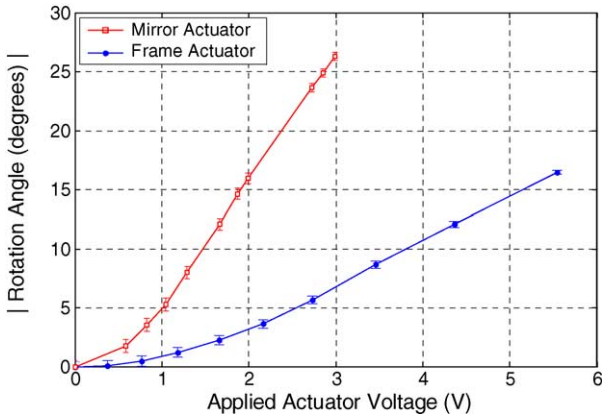


Fig. 6. Mechanical dc rotation angle vs. applied voltages for the two actuators. Absolute values are shown since rotation by the mirror actuator is considered positive, while rotation by the frame actuator is negative.

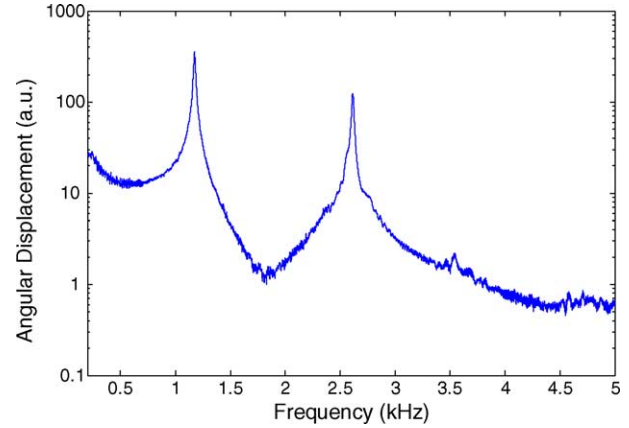


Fig. 8. Frequency response of the LVD micromirror device.

and it is also because the mechanical structure of the frame provides additional thermal isolation to the mirror actuator. The polysilicon resistance of the bimorph actuators change with applied voltage, and is plotted in Fig. 7(a). There is a large increase in the polysilicon resistance because its temperature coefficient of resistance is about  $5 \times 10^{-3} \text{ K}^{-1}$  [29]. The polysilicon resistance doubles when there is a temperature increase of 200 K. As evident from Fig. 7(b), there exists a linear correlation between the rotation angle and the polysilicon resistance for each of the two actuators. The resulting error (<2% of full-scale value) in fitting the actuator rotation and resistance data to a linear plot is within the experimental error of the rotation angle measurement. This linear relationship allows for independent control of rotation angle of each actuator by monitoring its polysilicon heater resistance. Thermal coupling between the two actuators can also be accounted for by monitoring their individual polysilicon heater resistances.

Thermal imaging of a two-axis electrothermal micromirror was performed in [23], which determined that the center

of the bimorph actuators had the maximum temperature rise of about  $95^\circ\text{C}$  during actuation. However, the substrate remained at the ambient temperature. The LVD micromirror is expected to exhibit similar thermal characteristics.

The frequency response of the LVD micromirror was measured using a Polytec OFV-511 laser Doppler vibrometer. The result is shown in Fig. 8. Note that the laser vibrometer measures the vertical displacement of a chosen spot on the rotating mirror plate. So, the plot in Fig. 8 reflects the relative angular displacements of the mirror plate at different frequencies. The resonant peaks for the frame and mirror actuator structures were observed at 1.18 and 2.62 kHz, respectively. These results are a close match to the modes observed at 1.14 and 2.76 kHz from simulations using CoventorWare. When electrical current is passed only through the mirror actuator at its resonance, the mechanical resonance of the mirror structure (Q-factor of 25) generates large bi-directional scans. At its resonance frequency of 2.6 kHz, the optical angle scanned by the mirror ranges from  $27^\circ$  at a dc plus ac drive voltage of  $(0.15 + 0.3 \sin \omega t) \text{ V}$  to  $170^\circ$  at  $(0.6 + 0.6 \sin \omega t) \text{ V}$ . Opti-

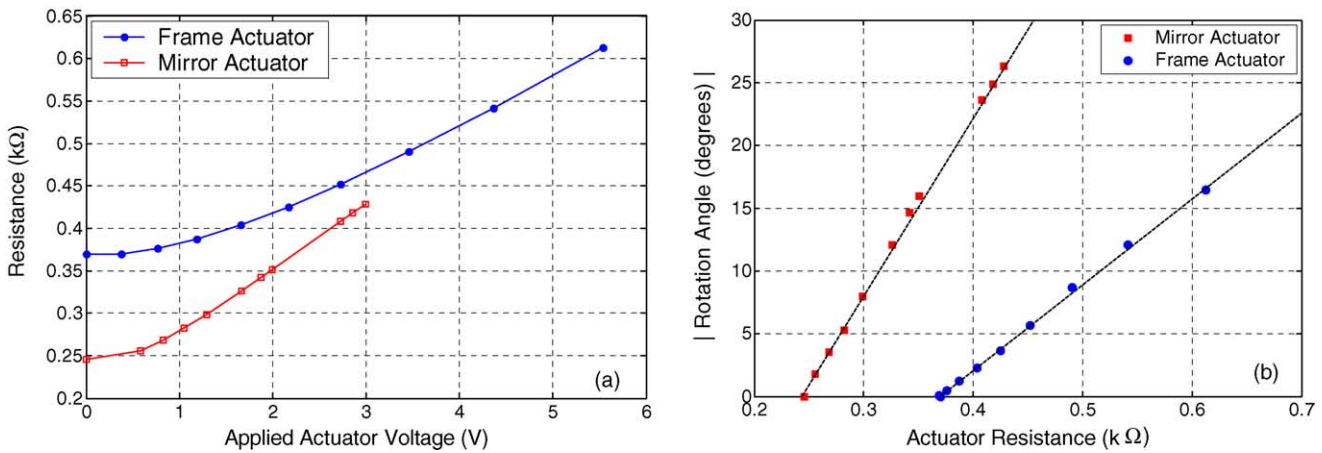


Fig. 7. Static response. (a) Actuator polysilicon resistances vs. applied voltage; (b) linear plot of rotation angle vs. actuator resistance for the two actuators.

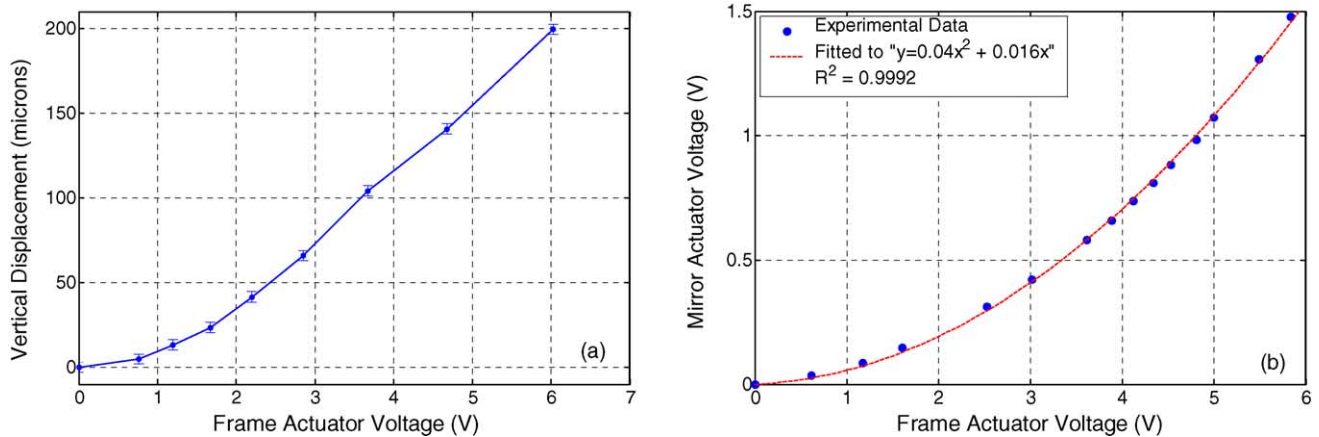


Fig. 9. Piston motion mode. (a) Vertical displacement of the mirror plate as a function of the frame actuator voltage; (b) plot of the mirror actuator voltage vs. corresponding frame actuator voltage that is required to maintain zero angular tilt of the mirror.

cal scan angles greater than  $170^\circ$  were observed visually at marginally higher voltages, but could not be monitored since the reflected light beam is blocked by the package sidewall. This large-angle scanning is stable and repeatable.

The thermal time response of the actuators is less than 0.4 ms, since the mirror is able to scan at a frequency of 2.6 kHz. This time response is adequate for the OCT imaging application that the mirror has been designed for. However, the thermal response time can be decreased further by reducing the thermal resistance of the bimorph actuators, but at the price of higher power consumption.

#### 4.2. Piston motion

Piston motion of the mirror can be achieved by equal but opposite angular rotations of the two actuators. By using the rotation angle versus applied voltage data, a mirror actuation voltage versus frame actuation voltage plot for same angular rotation values can be obtained. The slope of this experimentally determined plot provides the driving voltage ratio for the two actuators that would maintain zero tilting of the mirror plate. A voltage divider was used to drive the mirror and frame actuators with a voltage ratio of 3:7 (determined from experiment). A maximum vertical displacement of  $200\ \mu\text{m}$  was obtained. The vertical displacement of the mirror as a function of the drive voltage is shown in Fig. 9(a). By using the linearly fitted voltage ratio, the tilting of the mirror plate during the full vertical scan range is about  $1^\circ$ . Tilting of the mirror plate during actuation was recorded by monitoring the lateral displacement of the reflected laser beam by a quadrant photodetector.

To reduce this  $1^\circ$  tilting of the mirror plate during vertical piston motion, the two actuators are simultaneously actuated with the mirror actuator voltage supplied as a non-linear function of the frame actuator voltage, as shown in Fig. 9(b). This non-linear relationship between the two actuators can be fitted into a second-degree polynomial within 99.92%. A

maximum vertical displacement of  $200\ \mu\text{m}$  was once again obtained, but with less than  $0.03^\circ$  tilting of the mirror plate during the entire actuation range. This is a significant improvement over the  $1^\circ$  tilting that occurred when a linear voltage divider was used to drive the device [24]. Since the fabrication process is compatible with CMOS processes, control circuits for the two actuators can be integrated with the mirror on the same chip.

#### 5. Conclusions

A large vertical displacement micromirror with a novel electrothermal actuation mechanism was successfully demonstrated. The presented design uses a complementary configuration of two actuators for making micromirrors that are capable of high-speed vertical scanning as well as one-dimensional bi-directional rotational scanning. A maximum vertical displacement of  $200\ \mu\text{m}$  has been achieved with a microdevice of only  $0.7\ \text{mm} \times 0.32\ \text{mm}$  in size. Much larger vertical displacements in the millimeter-range can be achieved by simply increasing the length of the frame and/or the initial tilt angle of the frame. The fabrication process is simple and compatible with CMOS processes; therefore, control circuits can be integrated with the mirror on the same chip. The large actuation range and fast scanning speeds make this device very suitable for use in interferometry, laser beam steering, biomedical imaging, and phase modulation applications.

#### Acknowledgements

The authors would like to thank Ms. T. Riedhammer for her assistance with the SEM images. This work has been supported in part by the NASA UCF/UF Space Research Initiative and by the National Science Foundation Biophotonics Program under the award #0423557.

## References

- [1] P.F. Van Kessel, L.J. Hornbeck, R.E. Meier, M.R. Douglass, A MEMS-based projection display, in: *Proceedings of IEEE*, vol. 98, 1998, pp. 1687–1704.
- [2] D.M. Bloom, Grating light valve: revolutionizing display technology, in: *Proceedings of SPIE Projection Displays III*, vol. 3013, 1997, pp. 165–171.
- [3] H. Xie, Y. Pan, G.K. Fedder, Endoscopic optical coherence tomographic imaging with a CMOS-MEMS micromirror, *Sens. Actuators A* 103 (2003) 237–241.
- [4] D.L. Dickensheets, G.S. Kino, Micromachined scanning confocal optical microscope, *Opt. Lett.* 21 (1996) 764–766.
- [5] J.T. Nee, R.A. Conant, R.S. Muller, K.Y. Lau, Lightweight, optically flat micromirrors for fast beam steering, in: *IEEE/LEOS International Conference on Optical MEMS*, 2000, pp. 9–10.
- [6] J.J. Bernstein, W.P. Taylor, J.D. Brazzle, C.J. Corcoran, G. Kirkos, J.E. Odhner, A. Pareek, M. Waelti, M. Zai, Electromagnetically actuated mirror arrays for use in 3-D optical switching applications, *J. Microelectromech. Syst.* 13 (2004) 526–535.
- [7] M.A. Helmbrecht, U. Srinivasan, C. Rembe, R.T. Howe, R.S. Muller, Micromirrors for adaptive-optics arrays, in: *Technical Digest of the 11th International Conference on Solid State Sensors and Actuators (Transducers'01)*, Munich, Germany, June 10–14, 2001.
- [8] A.P. Lee, C.F. McConaghy, G. Sommargren, P. Krulvitch, E.W. Campbell, Vertical-actuated electrostatic comb drive with in situ capacitive position correction for application in phase shifting diffraction interferometry, *J. Microelectromech. Syst.* 12 (2003) 960–971.
- [9] S.-W. Chung, Y.-K. Kim, Design and fabrication of  $10 \times 10$  microspatial light modulator array for phase and amplitude modulation, *Sens. Actuators A* 78 (1999) 63–70.
- [10] S. Kwon, V. Milanovic, L.P. Lee, Vertical microlens scanner for 3D imaging, *Technical Digest of the 2002 Solid-State Sensor and Actuator Workshop*, Hilton Head Isl., SC, June 2002, pp. 227–230.
- [11] K. Sato, M. Shikida, Electrostatic film actuator with a large vertical displacement, in: *Proceedings of IEEE MEMS 1992*, Feb 4–7, 1992, pp. 1–5.
- [12] L.Y. Lin, J.L. Shen, S.S. Lee, M.C. Wu, Surface-micromachined micro-XYZ stages for free-space microoptical bench, *IEEE Photonics Technol. Lett.* 9 (1997) 345–347.
- [13] D. Huang, E.A. Swanson, C.P. Lin, J.S. Schuman, W.G. Stinson, W. Chang, M.R. Hee, T. Flotte, K. Gregory, C.A. Puliafito, J.G. Fujimoto, Optical coherence tomography, *Science* 254 (1991) 1178–1181.
- [14] J.M. Schmitt, Optical coherence tomography (OCT): a review, *IEEE J. Select. Top. Quant. Electron.* 5 (1999) 1205–1215.
- [15] Y. Pan, E. Lankenau, J. Welzel, R. Birngruber, R. Engelhardt, Optical coherence-gated imaging of biological tissues, *IEEE J. Selected Topics in Quantum Electronics* 2 (1996) 1029–1034.
- [16] K.F. Kwong, D. Yankelevich, K.C. Chu, J.P. Heritage, A. Dienes, 400-Hz mechanical scanning optical delay line, *Opt. Lett.* 18 (1993) 558–560.
- [17] X. Liu, M.J. Cobb, X. Li, Rapid scanning all-reflective optical delay line for real-time optical coherence tomography, *Opt. Lett.* 29 (2004) 80–82.
- [18] D. Lee, U. Krishnamoorthy, K. Yu, O. Solgaard, High-resolution, high-speed microscanner in single-crystalline silicon actuated by self-aligned dual-mode vertical electrostatic combdrive with capability for phased array operation, in: *Technical Digest of the 12th International Conference on Solid State Sensors, Actuators and Microsystems (Transducers'03)*, Boston, MA, June 8–12, 2003, pp. 576–579.
- [19] O. Cugat, P. Mounaix, S. Basroux, C. Divoux, G. Reyne, Deformable magnetic mirror for adaptive optics: first results, in: *IEEE 13th Annual International Conference on MEMS*, Miyazaki, Japan, January, 2000, pp. 485–490.
- [20] D.E. Glumac, W.P. Robbins, A planar unimorph-based actuator with large vertical displacement capability. I. Experiment, *IEEE Trans. Ultrason., Ferroelectr. Freq. Control* 45 (1998) 1145–1150.
- [21] A. Tuantranont, L.-A. Liew, V.M. Bright, W. Zhang, Y.C. Lee, Phase-only micromirror array fabricated by standard CMOS process, *Sens. Actuators A* 89 (2001) 124–134.
- [22] H. Xie, A. Jain, T. Xie, Y. Pan, G.K. Fedder, A single-crystal silicon-based micromirror with large scanning angle for biomedical applications, *CLEO Technical Digest*, Baltimore, MD, 2003.
- [23] A. Jain, A. Kopa, Y. Pan, G.K. Fedder, H. Xie, A two-axis electrothermal micromirror for endoscopic optical coherence tomography, *IEEE J. Select. Top. Quant. Electron.* 10 (2004) 636–642.
- [24] A. Jain, H. Qu, S. Todd, G.K. Fedder, H. Xie, Electrothermal SCS micromirror with large vertical displacement actuation, *Technical Digest of the 2004 Solid-State Sensor, Actuator and Microsystems Workshop*, Hilton Head Isl., SC, June 2004, pp. 228–231.
- [25] A. Jain, S. Todd, H. Xie, An electrothermally-actuated, dual-mode micromirror for large bi-directional scanning, in: *Technical Digest of the IEEE International Electron Devices Meeting (IEDM) 2004*, San Francisco, CA, Dec 13–15, 2004, pp. 47–50.
- [26] H. Xie, L. Erdmann, X. Zhu, K. Gabriel, G.K. Fedder, Post-CMOS processing for high-aspect-ratio integrated silicon microstructures, *J. Microelectromech. Syst.* 11 (2002) 93–101.
- [27] CoventorWare 2003 Reference Manual, Coventor Inc., Cary, NC.
- [28] MOSIS integrated circuit fabrication service, Marina del Rey, CA, <http://www.mosis.org>.
- [29] S.D. Senturia, *Microsystem Design*, Kluwer, Boston, 2001, p. 636.

## Biographies

**Ankur Jain** received his BE (Honors) degree in electrical and electronics engineering from the Birla Institute of Technology and Science (BITS), Pilani, India in 2000, and his MS degree in electrical engineering from the University of Florida, Gainesville in 2002. He is currently working towards a PhD degree at the Biophotonics and Microsystems Laboratory at the University of Florida, Gainesville. His research interests include the design, fabrication and packaging of CMOS MEMS devices for biomedical imaging, endoscopic optical coherence microscopy, and photonic devices.

**Hongwei Qu** received the BS and MS degree in electrical engineering from the Tianjin University, Tianjin, China in 1988 and 1993, respectively. From 1993 to 2000, he was a faculty member at the Electrical Engineering Department of Tianjin University, where he was involved in the research on semiconductor sensors. Mr. Qu is now pursuing the PhD degree at the Department of Electrical and Computer Engineering, University of Florida. His current research involves CMOS MEMS technology, focusing on the integrated CMOS inertial measurement units and micro mirrors.

**Shane Todd** received his BS degree (Magna Cum Laude) in electrical engineering from the University of Florida in 2003. As an undergraduate he participated in various projects in the areas of nano-particle research and semiconductor processing. He is currently working towards his MS degree in electrical and computer engineering from the University of Florida. His graduate research has involved the design and modeling of electrothermal MEMS devices.

**Huikai Xie** is an Assistant Professor at the Department of Electrical and Computer Engineering of the University of Florida. He received his MS in electro-optics from Tufts University in 1998, and PhD degree in electrical and computer engineering from Carnegie Mellon University in 2002. He also holds BS and MS degrees in electronic engineering from Beijing Institute of Technology. From 1992 to 1996, he was a faculty member of the Institute of Microelectronics at Tsinghua University, Beijing, working on various silicon-based chemical and mechanical sensors. He has published over 40 technical papers. His present research interests include micro/nanofabrication, integrated microsensors, optical MEMS and optical imaging.